Effective Forces Between Diamagnetic and Paramagnetic Ions in D 2 O at Low and Moderate Ionic Strengths: An NMR Relaxation Study

A. Sacco, E. Belorizky, M. Jeannin, W. Gorecki, P. Fries

J. Phys. II France **7** (1997) 1299–1322 SEPTEMBER **1997**, PAGE 1299

Effective Forces Between Diamagnetic and Paramagnetic Ions in D_2O at Low and Moderate Ionic Strengths: An NMR Relaxation Study

A. Sacco ([1]), E. Belorizky ([2]), M. Jeannin ([2]), W. Gorecki ([2]) and P.H. Fries ([3,*])

([1]) Dipartimento di Chimica, Università degli Studi, Via E. Orabona 4, 70126 Bari, Italy
([2]) Laboratoire de Spectrométrie Physique (**), Université Joseph Fourier/Grenoble 1, BP. 87, 38402 St Martin d'Hères, France
([3]) Département de Recherche Fondamentale sur la Matière Condensée, SCIB/RI, CEA Grenoble, 17 rue des Martyrs, 38054 Grenoble Cedex 9, France

(Received 14 February 1997, received in final form 9 May 1997, accepted 15 May 1997)

PACS.61.20.-p – Structure of liquids
PACS.66.10.-x – Diffusion and ionic conduction in liquids
PACS.76.60.-k – Nuclear magnetic resonance and relaxation

Abstract. — The dynamical behaviour of several pairs of dissociated, attractive and repulsive, ions is investigated in aqueous solutions for ionic strengths up to 1 mol l^{-1}. The experimental information is provided by the NMR longitudinal relaxation rates of the protons on the diamagnetic ions. The ionic solutions were chosen so that the main relaxation mechanism of these protons is due to the time fluctuations of their dipolar magnetic coupling with the electronic spins on the paramagnetic ions. This coupling strongly depends on the ion-ion potential of mean force (PMF) and on the ion self-diffusion coefficients. The interionic spatial correlations and the associated PMF are derived from a new approximation of the integral equations of the statistical mechanics of liquids. This formalism, which treats all the ions as discrete particles, rests on the infinite dilution PMF of the various ion pairs. It mixes a Born-Oppenheimer theory at infinite dilution with a sort of McMillan-Mayer approximation to take the ionic concentration into account. It goes beyond the Debye-Hückel screening theory, in which a continuous screening charge distribution approximates the effects of the discrete surrounding ions. It is related to the concept of the local dielectric constants which replace the usual macroscopic dielectric constant and depend on the interionic distances. The self-diffusion coefficients of the diamagnetic ions were measured by the NMR pulsed magnetic field gradient (PMFG) techniques applied to the resonant protons. In paramagnetic solutions, where several protonated species coexist, special caution is required and this is discussed in detail. For all the investigated solutions the theory well accounts for the observed variation of the NMR relaxation as a function of the ion charges, of the ionic strength and of the NMR proton resonance frequency. The relaxation results predicted by the new approximation of the ion-ion PMF are compared with those derived from the simple Debye-Hückel screening formalism, which can be reasonably used up to moderate ionic strengths.

(*) Author for correspondence (e-mail: fries@drfmc.ceng.cea.fr)
(**) CNRS-UMR 5588

Résumé. — On étudie la dynamique de plusieurs paires d'ions attractifs et répulsifs en solution aqueuse à des forces ioniques atteignant 1 mol l^{-1}. La mesure des taux de relaxation nucléaire longitudinale des protons des ions diamagnétiques fournit l'information expérimentale. On a choisi les solutions ioniques de sorte que le principal mécanisme de relaxation de ces protons soit les fluctuations temporelles de leur interaction dipolaire magnétique avec les spins électroniques des ions paramagnétiques. Cette interaction dépend fortement du potentiel des forces moyennes (PMF) ion-ion et des coefficients d'auto-diffusion ioniques. On calcule les corrélations spatiales ion-ion et les PMF associés à l'aide d'une nouvelle approximation des équations intégrales de la mécanique statistique des liquides. Ce formalisme traite tous les ions comme des particules discrètes. Il est fondé sur les PMF d'infinie dilution des différentes paires d'ions. Il mélange une théorie de Born-Oppenheimer pour la dilution infinie avec une approximation de type McMillan-Mayer pour tenir compte de la concentration ionique. Il va au-delà du modèle d'écrantage de Debye-Hückel où une distribution continue de charge rend compte des effets des ions discrets environnants. Il est relié au concept des constantes diélectriques locales qui généralisent la constante diélectrique macroscopique usuelle et sont fonction des distances ion-ion. On a mesuré les coefficients d'auto-diffusion des ions diamagnétiques par des techniques RMN de gradients pulsés de champ magnétique (PMFG), appliquées aux protons résonnants. Dans les solutions paramagnétiques contenant plusieurs espèces protonées, les précautions particulières à prendre sont discutées en détail. Dans toutes les solutions considérées la théorie rend bien compte des taux de relaxation en fonction des charges des ions, de leurs concentrations et de la fréquence de résonance des protons. On compare les résultats de relaxation prédits par la nouvelle approximation des PMF ion-ion à ceux déduits du formalisme d'écrantage coulombien simple de Debye-Hückel, qui s'applique encore assez bien jusqu'à des forces ioniques modérées.

1. Introduction

The relative equilibrium distribution and the relative motion of two particles in a liquid have been the subject of many NMR studies since 1953 [1]. The behaviour of uncharged, non polar particles is reasonably modelled [2, 3]. However, despite their practical use, polar molecules and ions show a much more complicated microdynamics, which is not yet well-understood and gives rise to increasing interest [4–10]. Measurements of the nuclear intermolecular longitudinal relaxation rates $R_1 = 1/T_1$ are one of the most suitable techniques for studying the relative distribution and motion of two particles in a liquid [8, 11, 12], since these rates are linear combination of the spectral densities of the time correlation functions of the fluctuating interspin position. Recently [13, 14], we reported careful measurements of the relaxation rates $R_{1S} = 1/T_{1S}$ of the protons and phosphorus nucleus on the tetramethylphosphonium (TMP^+) cation $(CH_3)_4P^+$ caused by the electronic spins S on the nitrosodisulfonate (NDS^{2-}) $^{\bullet}ON(SO_3)_2^{2-}$ free radical anions in D_2O solutions at 25 °C. The measurements were repeated for several NMR frequencies and various radical concentrations up to 0.08 mol l^{-1} The experimental results were interpreted using an ion-ion potential of mean force (PMF) calculated for a model of attractive hard ions in a solvent of discrete water-like polar polarizable molecules. The relaxation rates were calculated by assuming that the relative diffusion of the ions is given by the solutions of a Smoluchowski equation associated with the above PMF and by taking the eccentricity of the interacting spins into account. The agreement between theory and experiment was good for the proton relaxation without any adjustable parameter, but it was less satisfactory for the phosphorus relaxation.

However, several problems still remained both from the theoretical and experimental points of view. The theory, which applied to solutions of low ionic concentrations, should be extended

for higher ionic strengths. In our previous studies [13, 14], the direct anion-cation Coulomb potential in the D_2O solvent was screened by the other ions according to a Debye-Hückel (DH) type approximation [15a] as follows. We introduced the ion-ion PMF at infinite dilution, $w_{IS}^{ID}(R)$, which only depends on the properties of the two interacting ions and of the solvent. Then, we assumed that the corresponding PMF at finite concentration, $w_{IS}^{FC}(R)$, is the sum of the infinite dilution limit $w_{IS}^{ID}(R)$ and of a screening potential due to the continuous charge distribution formed by all the other ions around each of the interacting ions. In a complete *ab initio* theory all the ionic species surrounding the investigated ion pair and yielding the screening potential should be treated on the same grounds as the two studied ions and the water molecules. This can be done within the integral equation formalism [16, 17a], using coupled Ornstein-Zernike (OZ) relations and adequate closure equations for all pairs of species. This is a rather difficult task. A reasonable approximation based on the infinite dilution limits of the PMF and connected to the concept of local dielectric constants will be presented here.

For the considered nuclear frequencies the theoretical relaxation rates are nearly inversely proportional to the relative diffusion constant D of the two interacting ions. D is taken to be the sum of the self-diffusion coefficient D_I^t of the diamagnetic ion carrying the studied nuclei I and of the the self-diffusion coefficient D_S^t of the paramagnetic ion bearing the electronic spin S. These coefficients depend on the ion concentrations. Experimental values are available for the tetramethylammonium TMA^+ ion which is present in several D_2O solutions studied in this work. However, these values correspond either to dilute solutions, in which the self-diffusion constant can be derived from conductance data [18] using the Nernst-Einstein equation [19a–21] and the Onsager limiting law [23], or to solutions with rather high salt concentrations $\geq 1\,M$, where the TMA^+ translational diffusion has been studied by NMR spin echo techniques [21, 22]. Also note that the limiting self-diffusion of NDS^{2-} was measured by voltammetric investigation [24] in light water. Recent advances in the use of integral equation methods have allowed to compute the change of the self-diffusion coefficient of a given ion due to the surrounding ions for 1:1 electrolytes up to moderate concentrations [25]. Unfortunately, it is still impossible to predict the self-diffusion of a solute at infinite dilution in a solvent. Here, we report additional self-diffusion measurements performed in the intermediate concentration domain. The diffusion constants D_I^t were obtained through the usual pulse magnetic field gradient (PMFG) NMR method following a sequence proposed by Stejskal and Tanner [26]. Now, there are few published values for the diffusion coefficients of paramagnetic species. Indeed, these particles do not carry any resonating nucleus with a large natural abundance as the NDS^{2-} radical, and/or their resonating nuclei cannot be observed because of their very rapid intramolecular relaxation due to the electronic spin. Alternatives to the NMR technique are electrochemical methods, such as chronoamperometry. Unfortunately, the latter could not be applied to measure the self-diffusion of the NDS^{2-} anion, because of the interference signals of other electroactive diffusing ions in the solution. Finally, note that the self-diffusion constants of several organic free radicals have been recently obtained by modern laser techniques [27], which are not yet easily available. Here, we show how D_S^t can be estimated in an indirect way from NMR intermolecular relaxation data.

In this work the studied diamagnetic ions are the tetramethylammonium (TMA^+) cation $(CH_3)_4N^+$, the TMP^+cation and the methanesulfonate (MS^-) anion $CH_3SO_3^-$. The paramagnetic ions are the NDS^{2-} divalent radical anion and the hexahydrated manganous cation $Mn(D_2O)_6^{2+}$. We discuss the NMR results obtained for several pairs of both attractive and repulsive ions TMA^+/NDS^{2-}, TMP^+/NDS^{2-}, MS^-/NDS^{2-}, $TMP^+/Mn(D_2O)_6^{2+}$ in D_2O solutions at various ionic strengths.

The paper is organized as follows. Experimental details are given in Section 2. The new theory of the ion-ion PMF is developed in Section 3. The theoretical expression of the

intermolecular dipolar relaxation rate R_1 in terms of the PMF and of the molecular geometrical and dynamical properties is recalled in Section 4. In Section 5, the experimental results are displayed and discussed with respect to the theoretical hypotheses. The conclusion points out some of the questions which are still open.

2. Experimental

2.1. IONIC SOLUTIONS. — The solutions of tetramethylammonium chloride $(CH_3)_4NCl$ (Aldrich), tetramethylphosphonium chloride $(CH_3)_4PCl$ (Aldrich) and methanesulfonate $NaCH_3SO_3$ (Fluka) were made in very pure heavy-water (Eurisotop, 99.95 atom % D, sealed under argon). The hygroscopic ammonium salts were dried under vacuum at 80 °C in a Buchi oven in order to eliminate the light water, the proton signal of which is superimposed on that of the ammonium ions at low resolution. Paramagnetic potassium nitrosodisulfonate $K_2ON(SO_3)_2$ (Aldrich) was recrystallized in order to remove solid impurities and then dried under vacuum for approximately 48 h. The various salt concentrations were prepared by weighing the salts and the samples sealed in a dry box under argon. The nitrosodisulfonate NDS^{2-} concentrations were tested by measuring the solution absorbance in the visible spectrum at 540 nm using a Perkin-Elmer spectrometer. Sodium carbonate Na_2CO_3 was added to the NDS^{2-} solutions because the carbonate gives a basic solution, which stabilizes the NDS^{2-} radical that rapidly decomposes in neutral or acidic solution. It was found that 0.05 M of Na_2CO_3 is sufficient to stabilize the NDS^{2-} radicals in solution for approximately 2-3 days at 25 °C, and for about 1 week if the solution is kept frozen. The paramagnetic manganous solutions were prepared using manganous chloride $MnCl_2$ (Aldrich) and made slightly acidic in order to avoid the formation of insoluble brown manganous hydroxide. Of course, no Na_2CO_3 was added in this case.

2.2. NMR MEASUREMENTS. — Two kinds of proton NMR experiments were performed: (i) the relaxation times T_1 were measured at various frequencies; (ii) the self-diffusion coefficients were determined for the studied diamagnetic ions. The T_1 experimental values were obtained by the usual $180°-\tau-90°$ inversion recovery pulse sequence [28] with an accuracy better than 5%. The self-diffusion constants were deduced from the PMFG technique with the same precision.

For all solutions, where the equivalent protons of a single diamagnetic ionic species dominate the NMR signal, the above measurements can be performed with a low resolution spectrometer. But, when NMR signals originating from several species overlap, high resolution spectrometers must be used.

The low resolution experiments were performed with a Bruker CXP-100 spectrometer working at various frequencies in Grenoble and with a Bruker Minispec pc120 in Bari. The high resolution experiments were carried out with a Bruker AM-200 in Grenoble, and with a Tesla BS587 at 80 MHz and a Varian XL-200 in Bari.

2.3. SELF-DIFFUSION COEFFICIENTS

2.3.1. General Technique. — When only the proton signal of the studied diffusing ion was present in the spectrum, the self-diffusion coefficient was measured using a Bruker Minispec pc120 operating at 20 MHz and equipped with a PMFG accessory from Bruker itself. On the other hand, the FT-PGSE method was used on a Tesla BS587 high resolution NMR spectrometer working at 80 MHz and equipped with a pulsed field gradient probe consisting of anti-Helmholtz pair coils and of a current pulse generator from Stellar (Italy). All time durations were controlled by pulse programmer and all the parameters of the experiments by

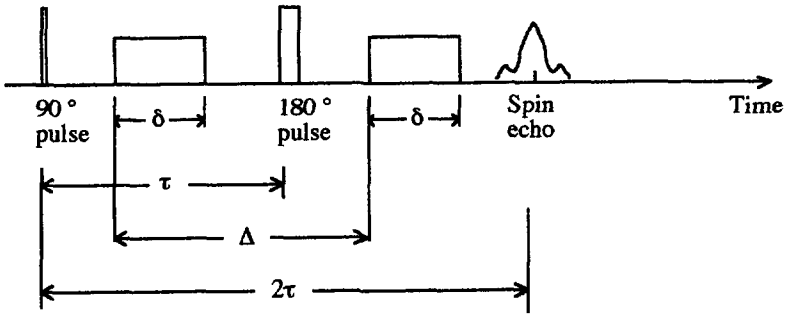

Fig. 1. — The time sequence of the pulsed magnetic field gradient (PMFG) used to measure the self-diffusion coefficients in the spin echo method.

computer, using the HROCH software. The measurements were performed with the magnetic field locked with ^2D external lock signal.

The pulse sequence suggested by Stejskal and Tanner [26] for the determination of self-diffusion coefficients is shown in Figure 1.

This technique measures molecular diffusion by probing the variation of the echo amplitude, using a $90°-\tau-180°-\tau$ echo pulse sequence, with two rectangular field gradient pulses which are superimposed on the static magnetic field and have magnitude G, separation time Δ and duration δ. At time 2τ, the echo reaches its maximum value and the data acquisition starts. After data acquisition, the spin echo signals are Fourier transformed into the frequency domain. The echo amplitude at time 2τ is

$$A^*(2\tau) = A(2\tau)\ \exp\left[(-\gamma_I G\delta)^2 \left(\Delta - \frac{\delta}{3}\right) D_I^t\right] \tag{1}$$

where γ_I is the proton magnetogyric ratio. $A(2\tau)$ is the amplitude of the echo observed without the field gradient. The self-diffusion coefficient was obtained by fitting the natural logarithm of the echo attenuation $\ln[A^*(2\tau)/A(2\tau)]$ to a linear function of $(-\gamma_I G\delta)^2 \left(\Delta - \frac{\delta}{3}\right)$. Most of the self-diffusion experiments were performed in Bari by calibrating the device from known self-diffusion coefficients of molecules such as dimethylsulphoxide, and by using time parameters such as $\Delta = 60\,\text{ms}$, $\tau = 60\,\text{ms}$ and δ varied from 1 ms to 13 ms by steps of 1 ms. Some of the measurements were also done in Grenoble using a near technique with a Bruker CXP-100 spectrometer and a home made field gradient unit. The temperature was regulated to $\pm 0.5\,\text{K}$ by a gaseous nitrogen flux. The parameters were $\Delta = 30\,\text{ms}$, $\tau = 30\,\text{ms}$, $\delta = 4\,\text{ms}$ and G was varied from 0 to $20\,\text{G cm}^{-1}$

2.3.2. Spurious Effects Due to HOD *Impurities.* — In a previous PMFG study at low NMR resolution [14,29], we observed a significant rise of the self-diffusion constant D_I^t of the TMP^+ cation in heavy water as the concentration of free radicals NDS^{2-} is increased, though the solution viscosity does not show any measurable change. Surprisingly, for a radical concentration of 0.08 M, the measured value of D_I^t seemed to be doubled with respect to its value in the diamagnetic solution [29]. Here, we show that this was an artefact. Even in very pure D_2O (99.95 atom % D) solutions, there is a small concentration $\approx 0.1\,\text{M}$ of HOD molecules, the self-diffusion coefficients D_I' of which are twice as large as the value D_I^t of the TMP^+ ions. Furthermore, the transverse relaxation time T_2' of the HOD protons is much longer than the relaxation time T_2 of the TMP^+ protons. At low resolution the number of protons N

of TMP^+ and N' of HOD both contribute to the observed NMR signal. Thus, denoting the echo amplitudes with and without the applied magnetic field gradient G again by $A^*(2\tau)$ and $A(2\tau)$, it is easily shown that at a time 2τ

$$\ln\left[\frac{A^*(2\tau)}{A(2\tau)}\right] = \ln\left[\frac{e^{-\alpha D_I^t} + \lambda e^{-\alpha' D_I'}}{1+\lambda}\right] = -\alpha D_{obs} \tag{2}$$

where D_{obs} is the measured apparent self-diffusion constant,

$$\alpha = (\gamma_I G\delta)^2 \left[\Delta - \frac{\delta}{3}\right] \tag{3}$$

and

$$\lambda = \frac{N'}{N} \exp\left[2\tau\left(\frac{1}{T_2} - \frac{1}{T_2'}\right)\right]. \tag{4}$$

In a typical PMFG experiment, $2\tau = 60$ ms and T_2 decreases from 320 ms to 100 ms, when the free radical concentration c_S increases from 0.02 M to 0.08 M. According to equation (2), $D_{obs} = D_I^t$, if $\lambda \ll 1$, *i.e.* $N' \ll N$ provided that the exponential factor is of the order of unity. Now, λ increases both with the ratio N'/N and with c_S, since $1/T_2 \propto c_S$, $1/T_2' \propto c_S$. When $\lambda \gg 1$, $D_{obs} = D_I'$. Indeed, we observed a marked increase of D_{obs} with the free radical concentration and this effect was more pronounced for a 0.1 M solution of TMP^+ than for a 0.5 M solution since the ratio N'/N is five times smaller for the latter. To sum it up, using extremely pure heavy water is essential to obtain reliable self-diffusion constants of dilute solutes by low resolution NMR spectroscopy, if the transverse proton relaxation time of the studied solute is much shorter than that of the residual HOD. Moreover, at high resolution, if the NMR signals of the various diffusing species overlap, their transverse relaxation times should be taken into account, when analyzing the echo amplitudes.

2.3.3. Paramagnetic Ions. — As already discussed in the introduction the self-diffusion coefficient D_S^t of the NDS^{2-} free radical anion cannot be easily measured. We suggest to deduce it from the experimental relaxation time T_1 of the protons located on a repulsive ion, such as the methanesulfonate MS^- anion, of self-diffusion constant D_I^t. Consider the paramagnetic contribution R_{1S} to the total relaxation rate of the MS^- protons due to their dipolar magnetic coupling with the electronic spins S on the NDS^{2-} radical. The theoretical expression of R_{1S}, recalled in Section 4, shows that this rate is roughly inversely proportional to the relative diffusion constant D of the two ionic species. Due to their strong Coulomb repulsion, the ions MS^- and NDS^{2-} remain far away from each other most of the time. So their relative microdynamics is rather insensitive to the structure of their hydration shells and to the discrete nature of the surrounding ions. In a first approximation their relative motion is mainly that of diffusing screened repulsive charged species in a dielectric continuum. Any simple model of the ions and of their relative motion, which takes this electrostatic repulsion properly into account, should apply. For instance, if the ions are approximated as charged hard spheres, the theoretical expression of R_{1S} is easily computed [30] as a function of D. D is then deduced by fitting the theoretical values of R_{1S} to its experimental counterparts. Assuming that $D = D_I^t + D_S^t$ is the sum of the self-diffusion constants of the repulsive ions and having measured the self-diffusion constant D_I^t of MS^- by the PMFG technique, D_S^t is derived by simple subtraction. As the accuracies of D and D_I^t are of the order of 5-10%, the uncertainty on D_S^t is about 10%. Note that this method obviously extends to the determination of the self-diffusion of a paramagnetic cation interacting with another repulsive diamagnetic cation, carrying the resonating protons.

3. Liquid Theory

3.1. THE DEBYE-HÜCKEL SCREENING LIMIT. — Consider two spherical ions i and j with charges q_i, q_j, and diameters d_i, d_j. Let $d_{ij} = (d_i + d_j)/2$ be their hard sphere collision diameter. Denote the distance between their centres by R. Assume that these ions and all the other surrounding ions are fully dissociated [20] in a solvent of macroscopic dielectric constant ε. In our previous works [13, 14, 30], the finite concentration (FC) potential of mean force $w_{ij}^{FC}(R)$ between the ions was given by

$$w_{ij}^{FC}(R) = \begin{cases} \infty & \text{if } R < d_{ij} \\ w_{ij}^{ID}(R) + \dfrac{q_i q_j}{\varepsilon R}\left[\dfrac{\exp\left[-\kappa(R-d_{ij})\right]}{1+\kappa d_{ij}} - 1\right] & \text{if } R \geq d_{ij} \end{cases} \tag{5}$$

where w_{ij}^{ID} is the infinite dilution (ID) limit of the ion-ion PMF and κ the inverse of the Debye screening length defined as

$$\kappa = \left(\frac{8\pi e^2 N_A \hat{I}}{1000 k_B T \varepsilon}\right)^{1/2} \tag{6}$$

N_A is the Avogadro number and $\hat{I} = \frac{1}{2}\sum_k c_k z_k^2$ is the ionic strength ot the solution, where the summation runs over all the ionic species k of concentrations c_k in mol l^{-1} and of valences z_k. The second term in the expression (5) for $R \geq d_{ij}$ represents the screening of the infinite dilution interaction w_{ij}^{ID} due to all the other ions which, following the Debye-Hückel model, are treated as a continuous charge distribution, called the ionic atmosphere. It is well-known that such a simple theory is appropriate for describing the long-ranged effects of the ionic atmosphere on w_{ij}^{ID}. However, it only represents a first approach of the short-ranged interionic spatial correlations. Therefore, the Debye-Hückel screening limit, expressed by the term in brackets of equation (5), is expected to be accurate only for solutions of dispersed ions, *i.e.* at low ionic strengths $\hat{I} \leq 0.1$ M.

Now, turn to solutions involving several ionic species at higher concentrations. The short range ion-ion spatial correlations must be treated by considering the ions as individual particles, with given sizes, shapes and charges, and no longer as a continuous charge distribution. In a water solution containing several ionic species, a full integral equation theory [31, 32] would combine the ion-ion, ion-water, and water-water correlations on an equal footing. This would lead to a large number of coupled OZ relations between pair correlation functions involving water. Since water is an anisotropic polar molecule, these functions are rather complicated. Indeed, they depend not only on the distance of the interacting particles, but also on the angles describing their relative orientation.

Here, we propose a simplified integral equation theory, beyond the Debye-Hückel approximation. Our main physical assumption is that the water-water and water-ion pair correlation functions of the infinite dilution limit are not modified by the presence of finite ionic concentrations. Obviously, this hypothesis requires that the numerical density of all the ions remains much smaller than that of water. It should apply for moderate ionic concentrations ≤ 1 M. Our procedure for calculating the ion-ion PMF w_{kl}^{FC} at moderate ionic concentrations rests on the preliminary knowledge of all the interionic effective potentials w_{kl}^{ID} at infinite dilution, where k, l run over all the ionic species. The computation of w_{kl}^{ID} needs to calculate the ion-water correlation functions, which in turn depend on the water-water spatial correlations. This is performed in three steps as follows.

3.2. THE INTERIONIC EFFECTIVE POTENTIAL w_{ij}^{ID} AT INFINITE DILUTION. — In this work, the infinite dilution PMF w_{ij}^{ID} is computed using the reference hypernetted chain (RHNC) approximation. Computational details were given in references [13,30]. Only the main lines of the derivation are sketched here.

3.2.1. Water-Water Correlation Functions. — Each water molecule is modelled by a hard sphere of diameter $d_w = 2.8$ Å, with an embedded central polarizable dipole and a tetrahedral quadrupole [33]. The dipole, quadrupole and dipolar polarizability have their experimental values. For the small and moderate ionic concentrations studied here, the number density of the water molecules ρ_w is assumed to be independent of the presence of the ions and has the value of the pure water at 25 °C. Denote the coordinates of position and orientation of a molecule by numbers such as 1, 2, 3. The direct and indirect water-water correlation functions $c_{ww}(12)$ and $\eta_{ww}(12)$ are computed as the solution of the OZ relation coupled with the reference linearized hypernetted chain (RLHNC) approximation [33]. The OZ relation is

$$\eta_{ww}(12) = \frac{\rho_w}{8\pi^2} \int c_{ww}(13)\,[c_{ww}(32) + \eta_{ww}(32)]\,d3 \tag{7}$$

where the integration is over all the possible positions and orientations 3 of a water molecule. Introduce a reference liquid, made of neutral hard spheres with the same volumes and number density as water. Its properties are denoted by the index r. Its pair correlation functions c_{rww}, η_{rww} and its pair distribution g_{rww} are assumed to be accurately known. The RLHNC closure can be written as [33]

$$c_{ww} = c_{rww} + g_{rww}\left[\frac{-U_{EL,ww}}{k_B T} + \eta_{ww} - \eta_{rww}\right] - (\eta_{ww} - \eta_{rww}) \tag{8}$$

where $U_{EL,ww}$ is the electrostatic potential between two polarizable water molecules. The simple RLHNC theory was used, since it leads at 25 °C to a theoretical dielectric constant of water $\varepsilon = 77.5$ in excellent agreement with the experimental value 78.5. This ensures an accurate treatment of the long range Coulomb forces between the ions.

3.2.2. Ion-Water Correlation Functions. — Consider a spherical ionic species i. In the infinite dilution limit, the direct and indirect ion-water correlation functions $c_{iw}(12)$ and $\eta_{iw}(12)$ are computed independently of the presence of the other ionic species j [13,34]. They are a solution of the OZ relation

$$\eta_{iw}(12) = \frac{\rho_w}{8\pi^2} \int c_{iw}(13)\,[c_{ww}(32) + \eta_{ww}(32)]\,d3 \tag{9}$$

and of the RLHNC closure

$$c_{iw} = c_{riw} + g_{riw}\left[\frac{-U_{EL,iw}}{k_B T} + \eta_{iw} - \eta_{riw}\right] - (\eta_{iw} - \eta_{riw})\,. \tag{10}$$

Here, the index r refers to a reference liquid, made of a neutral sphere having the same volume as the ion of species i and immersed in the reference liquid of neutral water described in Section 3.2.1. $U_{EL,iw}$ is the electrostatic potential between the ion and a polarizable water molecule.

3.2.3. Ion-Ion Correlation Functions. — At infinite dilution, the indirect correlation function η_{ij} between two spherical ionic species i and j is directly computed from the ion-water correlations using the OZ relation

$$\eta_{ij}\left(\|\mathbf{R}_2-\mathbf{R}_1\|\right)=\frac{\rho_w}{8\pi^2}\int c_{iw}(13)\left[c_{wj}(32)+\eta_{wj}(32)\right]\mathrm{d}3 \tag{11}$$

where $R=\|\mathbf{R}_2-\mathbf{R}_1\|$ is just the distance between the ion centres. The RHNC closure [13], allowing to calculate $w_{ij}^{ID}(R)$, is

$$w_{ij}^{ID}(R)=w_{rij}^{ID}(R)+U_{EL,ij}(R)-k_BT\left[\eta_{ij}(R)-\eta_{rij}(R)\right] \tag{12}$$

where $w_{rij}^{ID}(R)$, $\eta_{rij}(R)$ are the reference PMF and indirect correlation function between two neutral spheres, having the same volumes as the ionic species i and j, and immersed in the reference liquid of neutral water described in Section 3.2.1. $U_{EL,ij}$ is the Coulomb potential between the ions *in vacuo*.

3.3. The Interionic Effective Potential w_{ij}^{FC} at Moderate Concentrations. — Consider two spherical ions of species i and j, which are very distant from all the other ions in an extremely dilute solution. According to Section 3.2, their effective potential $w_{ij}^{ID}(R)$ can be calculated by using the three step procedure defined by equations (7) to (12). This infinite dilution potential is very simple, since it depends only on the interionic distance R. Now, turn to solutions containing several ionic species at finite concentrations. In our new theory, we assume that the water-water and water-ion pair correlation functions of the infinite dilution limit are conserved, still when there are ions up to moderate concentrations in the solution. The effective *direct* potential between the i and j species remains $w_{ij}^{ID}(R)$, even in the presence of other near ions. Our first theoretical treatment consists in applying the hypernetted chain (HNC) theory to the mixture made of the sole ions interacting by their effective *isotropic* potentials $w_{ij}^{ID}(R)$. The second theoretical treatment rests on the RHNC approximation applied to the same system.

3.3.1. The HNC Approximation of the Purely Ionic Mixture. — The finite concentration HNC-PMF w_{ij}^{FC} is defined as

$$w_{ij}^{FC}(R)=\begin{cases}\infty & \text{if } R<d_{ij}\\ w_{ij}^{ID}(R)-k_BT\eta_{ij}^{ion}(R) & \text{if } R\geq d_{ij}\end{cases} \tag{13}$$

η_{ij}^{ion} is the indirect correlation function between two ions of species i and j. It accounts for the effects of all the other ions on the spatial correlation of the two studied ions, but not for the hydration effects due to the discrete water molecules, which are already incorporated in the infinite dilution potential w_{ij}^{ID}. The HNC indirect correlation functions η_{ij}^{ion} are computed together with the HNC direct correlations c_{ij}^{ion} as the solution of the system of the coupled OZ relations

$$\eta_{ij}^{ion}(R)=\sum_k\rho_k\int c_{ik}^{ion}\left(\|\mathbf{R}_3-\mathbf{R}_1\|\right)\left[c_{kj}^{ion}\left(\|\mathbf{R}_2-\mathbf{R}_3\|\right)+\eta_{kj}^{ion}\left(\|\mathbf{R}_2-\mathbf{R}_3\|\right)\right]\mathrm{d}\mathbf{R}_3 \tag{14}$$

with $R=\|\mathbf{R}_2-\mathbf{R}_1\|$, and of the HNC closures

$$c_{ij}^{ion}(R)=\exp\left[-\frac{w_{ij}^{ID}(R)}{k_BT}+\eta_{ij}^{ion}(R)\right]-1-\eta_{ij}^{ion}(R) \tag{15}$$

where ρ_k is the number density of the ionic species k. Note that the ion-ion correlation functions are radial functions. They are much simpler than their counterparts which involve anisotropic water and depend on the angular variables that define the relative orientation of a water molecule with respect to an ion or to another water molecule. The η^{ion} functions are convolution products only over the ion position $d\mathbf{R}_3$ in equation (14). On the other hand, the integrals are over $d3 = d\mathbf{R}_3 d\Omega_w$ in the OZ relations (7), (9), (11), which account for the indirect spatial correlations through the water molecules of orientations Ω_w. Thus, the computational effort for solving the system of equations (14) and (15) is considerably reduced with respect to that needed for a solution containing anisotropic particles such as water. The theoretical treatment of several ionic species remains a simple numerical task.

3.3.2. The RHNC Approximation of the Purely Ionic Mixture. — Introducing a reference liquid allows a more accurate treatment of the short range spatial correlations between the molecules [35]. This is mainly used for dense liquids such as practical solvents of discrete molecules and ionic solutions in such solvents. In this paper, we shall examine the interest of a reference system, made of the sole ions, which are at moderate concentrations. The finite concentration RHNC-PMF w_{ij}^{FC} is defined as

$$w_{ij}^{\text{FC}}(R) = \begin{cases} \infty & \text{if } R < d_{ij} \\ w_{rij}^{\text{ion}}(R) + w_{ij}^{\text{ID}}(R) - k_B T \left[\eta_{ij}^{\text{ion}}(R) - \eta_{rij}^{\text{ion}}(R)\right] & \text{if } R \geq d_{ij} \end{cases} \tag{16}$$

where $w_{rij}^{\text{ion}}(R)$ and η_{rij}^{ion} are the PMF and the indirect correlation of two neutral hard spheres, having the same volumes as the ionic species i and j, and immersed in a mixture of hard spheres, the diameters and the numerical densities of which are those of the ions. The RHNC indirect correlation functions η_{ij}^{ion} are computed together with the RHNC direct correlations c_{ij}^{ion} as the solution of the system of the coupled OZ relations (14) and of the RHNC closures

$$c_{ij}^{\text{ion}}(R) = \exp\left[-\frac{w_{rij}^{\text{ion}}(R) + w_{ij}^{\text{ID}}(R)}{k_B T} + \eta_{ij}^{\text{ion}}(R) - \eta_{rij}^{\text{ion}}(R)\right] - 1 - \eta_{ij}^{\text{ion}}(R). \tag{17}$$

3.4. The Infinite Dilution Potential w_{ij}^{ID} and the Corresponding Local Dielectric Constant ε_{ij}. — The interionic PMF w_{ij}^{ID} has been derived in Section 3.2. It can be expressed in an equivalent and pictorial language by introducing a local dielectric constant $\varepsilon_{ij}(R)$, which depends on the ionic species i and j, and on the intercentre distance R. For $R \geq d_{ij}$, ε_{ij} is defined from w_{ij}^{ID} as

$$w_{ij}^{\text{ID}}(R) = \frac{q_i q_j}{\varepsilon_{ij}(R) R}. \tag{18}$$

At large distances, the effects of the discrete nature of the water molecules on w_{ij}^{ID} vanish so that $\varepsilon_{ij}(R) \to \varepsilon$. Then, $w_{ij}^{\text{ID}}(R)$ is nearly equal to the primitive model (PM) approximation defined as

$$w_{ij}^{\text{PM}}(R) = \begin{cases} \infty & \text{if } R < d_{ij} \\ \dfrac{q_i q_j}{\varepsilon R} & \text{if } R \geq d_{ij} \end{cases} \tag{19}$$

w_{ij}^{PM} is the well-known interaction between two charges in a dielectric continuum for $R \geq d_{ij}$. It is the simplest possible effective potential between two spherical ions in a polar solvent. From equations (18) and (19), we have

$$\frac{\varepsilon}{\varepsilon_{ij}(R)} = \frac{w_{ij}^{\text{ID}}(R)}{w_{ij}^{\text{PM}}(R)}. \tag{20}$$

4. Proton Relaxation Rates

The observed longitudinal relaxation rates $R_1 = 1/T_1$ of the protons in our solutions are

$$R_1 = R_1^0 + R_{1S} \tag{21}$$

R_1^0 is the proton longitudinal relaxation rate in the diamagnetic solution without paramagnetic species and R_{1S} the main contribution to the observed total rate due to the intermolecular interactions with the electronic spins S on the paramagnetic ions. The proton relaxation rate R_{1S} arises here from the dipolar magnetic coupling between the proton nuclear spin I and the electronic spins S. Contrarily to what is observed for the ^{31}P and ^{19}F nuclei, the scalar hyperfine coupling between the proton spin I and S is negligibly small. Indeed, there was no measurable shift of the resonance line of the protons due to their hyperfine coupling with added paramagnetic ions [13].

EPR spectra of the NDS^{2-} free radical [36] and of the Mn^{2+} transition cation [37, 38] in crystalline matrices have shown that their $\tilde{g}$ tensors are nearly isotropic. The electronic relaxation times T_{1e} and T_{2e} of the radical anion are of the order of 10^{-7} to 10^{-6} s [39], while those of the manganous cation in aqueous solution are of the order of 10^{-9} to 10^{-8} s [40]. On the other hand, the translational correlation time is close to 10^{-10} s in our solutions, *i.e.* much shorter than the electronic relaxation times. Then, the interaction of the protons with the electronic Curie spin is negligible [41, 42]. The proton relaxation arises from the random relative spatial motion of the interacting spins and not from the time fluctuations of S. The detailed theory giving the expression of R_{1S} was published previously [2,13,43–45]. Let N_S be the number density of the electronic spins. Let γ_I and γ_S be the magnetogyric ratios of the I and S spins located on the diamagnetic and paramagnetic interacting species, respectively. Denote the Larmor angular frequencies of these spins by ω_I and ω_S. As $\gamma_I \ll \gamma_S$, we have

$$R_{1S} = \frac{2}{5}\gamma_I^2\gamma_S^2\hbar^2 S(S+1)\frac{N_S}{\pi D b}\left[\bar{j}_2(\omega_I\tau) + \frac{7}{3}\bar{j}_2(\omega_S\tau)\right]. \tag{22}$$

Following the notation used in our previous papers [13,45], $b = d_{IS} = (d_I + d_S)/2$ is the minimal distance of approach of the centres of the two spherical interacting species of diameters d_I and d_S. $D = D_I^t + D_S^t$ is the relative diffusion constant of these species and $\tau = b^2/D$ their translational correlation time. The reduced spectral density $\bar{j}_2(\omega\tau)$ is a dimensionless quantity related to the dipolar spectral density $j_2(\omega)$ by

$$\bar{j}_2(\omega\tau) = \frac{\pi b^3}{N_S\tau} j_2(\omega). \tag{23}$$

The latter is the Fourier transform of the time correlation function $g_2(t)$ of the random functions $r^{-3}Y_{2q}(\theta,\phi)$ of the vector $\mathbf{r}(r,\theta,\phi)$, which joins the position of the spin I to that of the spin S. We have

$$j_2(\omega) = \frac{1}{2\pi}\int_{-\infty}^{+\infty} g_2(t)\mathrm{e}^{-i\omega t}\mathrm{d}t \tag{24}$$

and

$$g_2(t) = \left\langle r_0^{-3}Y_{2q}(\theta_0,\phi_0) \times \left[r^{-3}Y_{2q}(\theta,\phi)\right]^* \right\rangle. \tag{25}$$

The reduced spectral density $\bar{j}_2(\omega\tau)$ depends on the pair distribution $g_{IS}(R)$ of the two ions carrying the I and S spins. This distribution is defined in terms of the ion-ion PMF w_{IS}^{FC} as

$$g_{IS}(R) = \exp\left[-\frac{w_{IS}^{FC}(R)}{k_B T}\right]. \tag{26}$$

Following standard notations the same letter g is used both for the pair distribution $g_{IS}(R)$ [16, 17a], and for the time correlation function $g_2(t)$ [46]. $\bar{j}_2$ also depends on the rotational ionic diffusion constants D_I^r and D_S^r. Finally, it is a function of the eccentricity parameters $(p_I/b)^2$ and $(p_S/b)^2$, where p_I, p_S are the distances of I and S to the ion centres. It has been shown [44,45] that $j_2(\omega)$ can be expressed in a power series of the eccentricity parameters, the leading term of the series corresponding to the value $J_2(\omega)$ of $j_2(\omega)$, for which the spins are at the ion centres. In this case, the time correlation function $g_2(t)$ reduces to $G_2(t)$, which is the inverse Fourier transform of $J_2(\omega)$ and can be written as

$$G_2(t) = N_S \int\int g_{IS}(R_0)\rho(\mathbf{R}_0, \mathbf{R}, t) R_0^{-3} Y_{2q}(\Theta_0, \Phi_0) \times \left[R^{-3} Y_{2q}(\Theta, \Phi)\right]^* \mathrm{d}^3\mathbf{R} \qquad (27)$$

$\mathbf{R}_0(R_0, \Theta_0, \Phi_0)$ and $\mathbf{R}(R, \Theta, \Phi)$ are the intercentre vectors at time 0 and t, respectively. The conditional probability $\rho(\mathbf{R}_0, \mathbf{R}, t)$ accounts for the relative diffusion of the ions coupled by their PMF. It is a solution of the Smoluchowski diffusion equation discussed in references [2, 45]. $\bar{j}_2$ will be computed from equations (23) to (27), using the PMF w_{IS}^{FC} given in Section 3.3, according to the numerical procedure described in reference [45].

5. Results and Discussion

We have studied the dynamical behaviour of several pairs of attractive and repulsive ions in D_2O solutions at low and moderate ionic strengths. The investigated pairs are TMA^+/NDS^{2-}, TMP^+/NDS^{2-}, MS^-/NDS^{2-}, and $TMP^+/Mn(D_2O)_6^{2+}$, where TMA^+, TMP^+, MS^-, and NDS^{2-} denote the tetramethylammonium cation $(CH_3)_4N^+$, the tetramethylphosphonium cation $(CH_3)_4P^+$, the methanesulfonate anion $CH_3SO_3^-$, and the nitrosodisulfonate radical anion $^\bullet ON(SO_3)_2^{2-}$, respectively. The new theoretical treatment proposed in Section 3 will be worked out in detail for the ion pair TMA^+/NDS^{2-} For the other pairs, the results obtained by similar derivation will be only given.

5.1. The TMA^+/NDS^{2-} Attractive Pair. — The study of the microdynamics of this pair was carried out in heavy water solutions of tetramethylammonium chloride $(CH_3)_4NCl$, potassium nitrosodisulfonate $K_2ON(SO_3)_2$ and sodium carbonate Na_2CO_3. After dissociation of the various salts, we have the following ionic species: the studied TMA^+ and NDS^{2-} ions, Cl^-, K^+, Na^+, CO_3^{2-}, DCO_3^- and OD^-, the last two species coming from the acid base equilibrium of CO_3^{2-} and heavy water D_2O. The concentrations of the ions CO_3^{2-}, DCO_3^-, OD^- were calculated using the equilibrium constant $K_b = 2.1 \times 10^{-4}$ for the water proton transfer to the base CO_3^{2-} $K_b = 10^{-14}/K_{a_2}$, where K_{a_2} is the the second acidity constant of carbonic acid [19a]. We have: $[DCO_3^-] = 0.0031\,M$, $[OD^-] = 0.0031\,M$, $[CO_3^{2-}] = 0.0469\,M$. Each of the salts has concentration ranging between 0.05 and 0.5 M. Direct application of the integral equation method to all the ionic species would lead to 36 different direct ion-ion correlation functions, 36 indirect correlation functions, and 36 potentials of mean force! Now, the task can be simplified as follows. The investigated relaxation rate R_{1S} of the protons on the TMA^+ cation is a function of the PMF w_{IS}^{FC} between this cation and the NDS^{2-} anion, and of the self-diffusion coefficients D_I^t and D_S^t of these ions. D_I^t and D_S^t are experimental quantities, the accuracy of which can only be marginally improved. Our theoretical effort should be directed towards a good description of w_{IS}^{FC}. Now, this effective potential mainly depends on the hydration of the studied ions TMA^+ and NDS^{2-}, and on the dielectric screening of their direct Coulomb interaction by the numerous water molecules. The other surrounding ions are at low or moderate concentrations. They are not closely packed with the studied ions with which they mainly interact at medium and long range distances. The sizes, shapes and

internal electronic structures of the surrounding ions only play a secondary role. Therefore, all the surrounding ions with the same charge can be safely replaced by an effective ionic species carrying the same charge and having an effective volume. This effective volume is defined as the average of the volumes of the actual ions, weighted by their number densities. Now, the electrostatic attraction between a small cation and the water molecules of its first hydration shell is particularly strong. The life time of this hydration shell is expected to be longer than the characteristic time τ of the studied interionic dynamics. The volume of a small cation is then taken to be the volume of the hydrated entity rather than that of the bare ion. The number density of the effective ions is the sum of the number densities of the actual ions. For example, the Na^+ and K^+ hydrated ions with number densities $\rho(Na^+)$ and $\rho(K^+)$ and volumes $v(Na^+)$ and $v(K^+)$ are replaced by an unique species C^+ such as

$$\rho(C^+) = \rho(Na^+) + \rho(K^+) \tag{28}$$

and

$$v(C^+) = \frac{\rho(Na^+)v(Na^+) + \rho(K^+)v(K^+)}{\rho(C^+)} \tag{29}$$

Similarly, the anions Cl^-, DCO_3^-, OD^- are replaced by an unique species A^-, the number density $\rho(A^-)$ and effective volume $v(A^-)$ of which are defined as in equations (28) and (29). Finally, the number density and the volume of the unique surrounding divalent anionic species CO_3^{2-} are denoted by $\rho(A^{2-})$ and $v(A^{2-})$. Each of the effective ions $k = C^+$, A^-, A^{2-} are approximated as hard spheres with centred charges e, $-e$, $-2e$ and effective diameters

$$d_k = \left(\frac{6v_k}{\pi}\right)^{1/3} \tag{30}$$

To sum it up, we are led to a simpler model of the pair of interacting ions TMA^+ and NDS^{2-} in a bath made of discrete polar polarizable D_2O molecules and of three effective spherical ionic species $k = C^+$, A^-, A^{2-} with variable concentrations c_k. The diameters of TMA^+ and NDS^{2-} were chosen to be those of spheres having the same volumes as the CPK models of these ions. Similar estimations were done for the surrounding ions. Geometrical and dynamical parameters needed for the NMR calculations are summarized in Tables I and II.

Two sets of D_2O solutions containing 0.1 and 0.5 M of TMACl, both with 0.05 M of Na_2CO_3, were investigated at 298 K. The relaxation rates R_{1S} of the TMA^+ protons were measured at an NMR frequency $\nu_I = 200$ MHz. The experimental values are reported in Table III for concentrations of K_2NDS increasing from 0.01 to 0.08 M.

They are also displayed in Figure 2.

Now, consider the self-diffusion coefficients of the interacting ions. The diffusion of the diamagnetic TMA^+ cation was studied by the PMFG technique described in Section 2.3. As the K_2NDS concentration increases, the relative variation of the total number density of the ions is moderate inside both sets of TMACl solutions. So, inside each set of solutions, we did not measure any appreciable change of the self-diffusion coefficient of the TMA^+ cation, which was found to be $D_I^t = 0.89 \times 10^{-5}\,cm^2\,s^{-1}$ for the 0.1 M TMACl solution set and $D_I^t = 0.85 \times 10^{-5}\,cm^2\,s^{-1}$ for the 0.5 M TMACl solution set. The standard procedure, which is used throughout this work to determine self-diffusion coefficient D_S^t of a paramagnetic ion in a solution of moderate ionic strength, is now illustrated for the NDS^{2-} anion. At infinite dilution [24] in H_2O, the value of D_S^t is $1.48 \times 10^{-5}\,cm^2\,s^{-1}$ In our D_2O solutions containing finite electrolyte concentrations, it is estimated as follows. *Firstly, according to the Stokes-Einstein law, it is assumed to be inversely proportional to the solution viscosity* η, *which is*

Table I. — *Geometrical and dynamical parameters of the ions i carrying the interacting spins and approximated as hard spheres. d_i is the diameter of the ion and p_i the distance of the nuclear or electronic spin from the ion centre. D^t_{i0} is the translational self-diffusion coefficient of the ion at the infinite dilution limit. D^r_i is its rotational diffusion coefficient.*

ion i	d_i (Å)	p_i (Å)	D^t_{i0} (10^{-5} cm^2 s^{-1})	D^r_i (10^{10} s^{-1})
$(CH_3)_4N^+$	4.74	1.9	0.975[a]	3.3[a]
$(CH_3)_4P^+$	5.04	2.2	1.0[b]	2.8[b]
$(CH_3)SO_3^-$	4.48	1.6		3.3[c]
$^\bullet ON(SO_3)_2^{2-}$	5.15	1.6	1.2[a]	2.3[a]
$Mn(D_2O)_6^{2+}$	6.50	0.0	0.48[d]	

[a] Ref. [47]; [b] Ref. [13]; [c] the rotational diffusion constant of this monovalent anion is assumed to be that of the monovalent cation $(CH_3)_4N^+$ of nearly the same diameter; [d] Ref. [48]

Table II. — *Effective diameters d_k of the ions k, modelled by hard spheres, surrounding the ions which carry the interacting spins.*

ion k	hydrated Na^+	hydrated K^+	Cl^-	OD^-	DCO_3^-	CO_3^{2-}
d_k (Å)	7.5[a]	8.2[a]	3.6[a]	2.8[b]	3.9[c]	3.9[c]

[a] $d_k = 2(r_k + d_w)$ where r_k is the Pauling-Sherman radius of reference [15b], and $d_w = 2.8$ Å the diameter of the water molecules bound to the ion; [b] $d_k = d_w$; [c] from CPK models.

Table III. — *Measured relaxation rates R_1 of the $(CH_3)_4N^+$ protons for various concentrations c_S of $^\bullet ON(SO_3)_2^{2-}$ radicals in D_2O solutions at 298 K. The concentration of the stabilizer is $[Na_2CO_3] = 0.05\,M$. The proton resonance frequency is $\nu_I = 200\,MHz$.*

a) $[(CH_3)_4NCl] = 0.1$ M

$K_2ON(SO_3)_2$ concentration c_S (M)	0	0.02	0.03	0.04	0.06	0.08
proton relaxation rate R_1 (s^{-1})	0.116	9.82	13.31	18.85	26.2	33.15

b) $[(CH_3)_4NCl] = 0.5$ M

$K_2ON(SO_3)_2$ concentration c_S (M)	0	0.01	0.02	0.03	0.04	0.06	0.08
proton relaxation rate R_1 (s^{-1})	0.118	4.06	7.825	11.84	15.94	22.45	29.45

nearly equal to that of pure D_2O. Since the viscosity ratio $\eta(D_2O)/\eta(H_2O) = 1.23$, the self-diffusion coefficient of the NDS^{2-} anion decreases to 1.20×10^{-5} cm^2 s^{-1} in the D_2O solutions because of solvent viscosity effects. Secondly, although it is a rather rough approximation [25], the relative variation of the NDS^{2-} self-diffusion constant with respect to its infinite dilution value is taken to be that of a *reference ion* in the solution, such as TMA^+ More precisely,

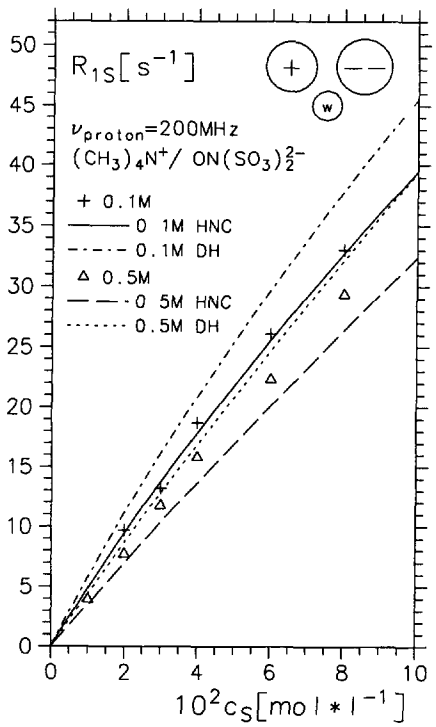

Fig. 2. — Measured intermolecular relaxation rates R_{1S} of the protons on the $(CH_3)_4N^+$ ions *versus* the concentration c_S of the $^{\bullet}ON(SO_3)_2^{2-}$ radical anions in D_2O solutions at 298 K for a proton resonance frequency $\nu_I = 200$ MHz. The results shown correspond to two solution sets containing 0.1 M and 0.5 M of $(CH_3)_4NCl$. The curves represent the theoretical relaxation rates computed from the potentials of mean force of the HNC and Debye-Hückel (DH) approximations.

denoting the diffusion coefficients of TMA^+ and NDS^{2-} by D^t_{I0} (see [21]) and D^t_{S0} in the infinite dilution limit, we have

$$D^t_S = \frac{D^t_I}{D^t_{I0}} D^t_{S0} \tag{31}$$

so that $D^t_S = 1.09 \times 10^{-5}\,cm^2\,s^{-1}$ in the 0.1 M TMACl solution set and $D^t_S = 1.04 \times 10^{-5}\,cm^2\,s^{-1}$ in the 0.5 M TMACl solution set. Note that the translational correlation time τ defined in Section 4 is 1.23×10^{-10} s and 1.28×10^{-10} s in the solution sets containing 0.1 and 0.5 M of TMACl, respectively. These are typical values for the solutions considered in this paper.

The HNC approximation proposed in Section 3.3.1 leads to the theoretical curves shown in Figure 2. Without any adjustable parameter the agreement with experiment is almost perfect for the solution set containing 0.1 M of TMACl. The deviations from the measured data do not exceed 10% for the 0.5 M solutions. This is at the limit of the error bars, to which each of the measured R_{1S} and D values involved in the theoretical expression (22) of R_{1S} amounts to 5%. This is a very satisfactory result, but it should be noted that the new HNC curve only represents a slight improvement with respect to the Debye-Hückel screening results, also plotted in Figure 2. For the ion-ion microdynamics, this shows that the Debye-Hückel screening model, which was previously expected to be limited to dilute ionic solutions, still applies up to

Table IV. — *Frequency dependence of the measured relaxation rates R_1 of the protons on the $(CH_3)_4P^+$ ions for various concentrations c_S of $^{\bullet}ON(SO_3)_2^{2-}$ radicals in D_2O solutions at 298 K. The concentrations of the diamagnetic salts are: $[(CH_3)_4PCl] = 0.5\ M$ and $[Na_2CO_3] = 0.05\,M$. The proton resonance frequencies are $\nu_I = 20$ and $80\,MHz$.*

a) $\nu_I = 20\,\text{MHz}$

$[K_2ON(SO_3)_2]$ (M)	0	0.015	0.020	0.029	0.046	0.060	0.062	0.072	0.095
R_1 (s^{-1})	0.120	13.16	13.7	19.6	29.4	33.3	37.0	41.7	58.8

b) $\nu_I = 80\,\text{MHz}$

$[K_2ON(SO_3)_2]$ (M)	0	0.021	0.04	0.06	0.08
R_1 (s^{-1})	0.120	10.3	20.0	28.6	37.45

ionic strengths of the order of 1 M. Indeed, the discrepancy with experiment for this simple approach remains below 15% in all the solutions.

5.2. The TMP^+/NDS^{2-} Attractive Pair. — This ion pair was already investigated in a solution of 0.1 M of TMPCl in heavy water at 298 K. To this end, the relaxation rate R_{1S} of the TMP^+ protons, caused by their coupling with the electronic spins S on the NDS^{2-} anions, was measured. The experiments were carried out at proton frequencies $\nu_I = 13$, 26, 80 MHz, and interpreted using the Debye-Hückel approximation for calculating the finite concentrations PMF [13]. Here, a D_2O solution with an intermediate concentration of 0.5 M of TMPCl is studied at 298 K. The concentration of the Na_2CO_3 stabilizer is again 0.05 M and the concentration of K_2NDS varies between 0 and 0.1 M. The experimental relaxation rates R_{1S}, which were measured at $\nu_I = 20$ and 80 MHz, are given in Table IV.

Geometrical and dynamical parameters of the various ions involved in the solutions are summarized in Tables I and II. The TMP^+ self-diffusion coefficient, measured by the PMFG technique, is $D_I^t = 0.80 \times 10^{-5}\,cm^2\,s^{-1}$. The NDS^{2-} self-diffusion coefficient was determined according to the procedure of Section 5.1, in which the reference diamagnetic ion is TMP^+ We have $D_S^t = 0.96 \times 10^{-5}\,cm^2\,s^{-1}$. The experimental relaxation rates are compared with the results of the HNC theory of Section 3.3.1 in Figure 3.

An excellent agreement is observed at 20 MHz, while the discrepancy at 80 MHz is lower than 15%.

5.3. The MS^-/NDS^{2-} Repulsive Pair. — We are now interested in the relative microdynamics of repulsive ions, such as $CH_3SO_3^-$ and $^{\bullet}ON(SO_3)_2^{2-}$. These ions were chosen in order to provide a direct comparison of the effects of repulsive Coulomb forces on the relaxation rates with those of attractive Coulomb forces. Indeed, the MS^- anion and the TMA^+ cation have nearly the same volumes. The comparative NMR study of the pairs MS^-/NDS^{2-} and TMA^+/NDS^{2-} in the same solution will probe the influence of the sign of the Coulomb potential.

We prepared mixed D_2O solutions containing 0.12 M of NaMS, 0.5 M of TMACl, 0.05 M of Na_2CO_3, and variable concentrations of K_2NDS. The relaxation rates of the methyl protons on both the MS^- and TMA^+ ions were simultaneously measured at 298 K, using a high resolution spectrometer working at a proton resonance frequency $\nu_I = 200$ MHz. Their values are reported in Table V.

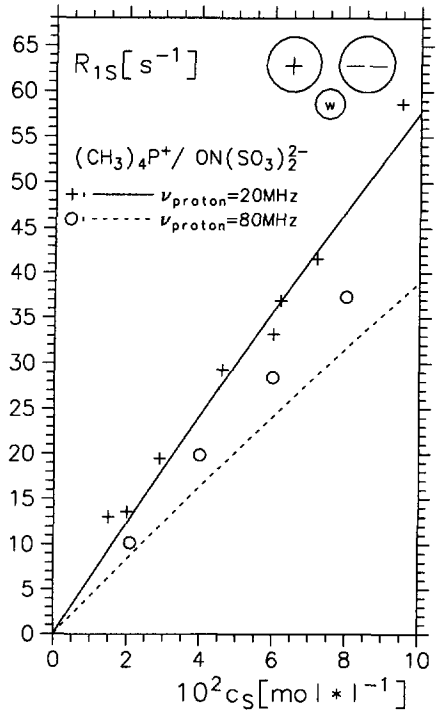

Fig. 3. — Frequency dependence of the measured intermolecular relaxation rates R_{1S} of the protons on the $(CH_3)_4P^+$ ions *versus* the concentration c_S of the $^{\bullet}ON(SO_3)_2^{2-}$ radical anions in D_2O solutions at 298 K. The concentration of $(CH_3)_4PCl$ is 0.5 M. The corresponding theoretical HNC values of Section 3.3.1 are represented by continuous and dashed lines at the proton resonance frequency $\nu_I = 20$ and 80 MHz, respectively.

Table V. — *Measured relaxation rates R_1 of the protons on the $(CH_3)_4N^+$ and $CH_3SO_3^-$ ions for various concentrations c_S of $^{\bullet}ON(SO_3)_2^{2-}$ radicals in D_2O solutions at 298 K. The concentrations of the diamagnetic salts are: $[(CH_3)_4NCl] = 0.5\,M$, $[NaCH_3SO_3] = 0.12\,M$ and $[Na_2CO_3] = 0.05\,M$. The proton resonance frequency is $\nu_I = 200\,MHz$.*

$K_2ON(SO_3)_2$ concentration c_S (M)	proton relaxation rate R_1 (s^{-1})	
	$(CH_3)_4N^+$	$CH_3SO_3^-$
0	0.118	0.20
0.011	3.88	1.12
0.022	7.75	2.12
0.033	9.90	2.72
0.044	15.4	4.27
0.055	19.6	5.65

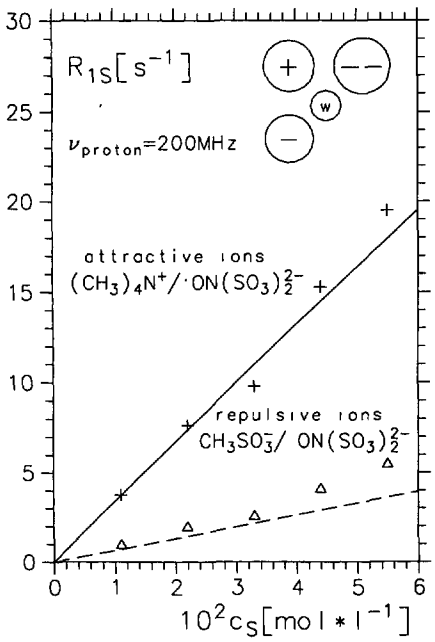

Fig. 4. — Comparison of the proton intermolecular relaxation rates R_{1S} between attractive and repulsive ions of nearly equal sizes in D_2O solutions at 298 K. For a proton resonance frequency $\nu_I = 200$ MHz, the relaxation rates of the $(CH_3)_4N^+$ and $(CH_3)SO_3^-$ protons are reported for various concentrations c_S of the $^{\bullet}ON(SO_3)_2^{2-}$ radical anions. The continuous and dashed lines represent the theoretical values calculated from the HNC potentials of mean force of Section 3.3.1.

Geometrical and dynamical parameters of the various ions involved in the solutions are summarized in Tables I and II. The self-diffusion constants of the diamagnetic ions were measured by the PMFG technique. They are: $D_I^t[TMA^+] = 0.85 \times 10^{-5}\,cm^2\,s^{-1}$ and $D_I^t[MS^-] = 0.89 \times 10^{-5}\,cm^2\,s^{-1}$ The NDS^{2-} self-diffusion coefficient was determined according to the procedure of Section 5.1 from the concentration dependence of the self-diffusion constant of TMA^+ It is $D_S^t = 1.04 \times 10^{-5}\,cm^2\,s^{-1}$

The comparison between the experimental relaxation rates and the HNC theoretical results, calculated according to the PMF approximation proposed in Section 3.3.1, are shown in Figure 4.

Again, an excellent overall agreement is observed for both the attractive and repulsive ion pairs. However, the theoretical relaxation rates for the MS^-/NDS^{2-} pair are slightly above the experimental values. This can be explained by the position of the negative charge of the $CH_3SO_3^-$ anion, mainly located on the oxygen atoms which are opposite the relaxing methyl protons. The methyl group is less pushed away from the NDS^{2-} anion by the actual negative charge on $CH_3SO_3^-$ than if this ion would carry a central negative charge as in our simple molecular model. Shorter distances between the protons and the electronic spin are allowed in real solutions. The spin-spin dipolar interactions are stronger and the experimental relaxation rate is greater than the theoretical prediction. Here, this type of discrepancy is favoured because, as shown hereafter, the MS^-/ NDS^{2-} Coulomb repulsion is notably screened, by the numerous surrounding ions which are dissolved in these rather concentrated solutions.

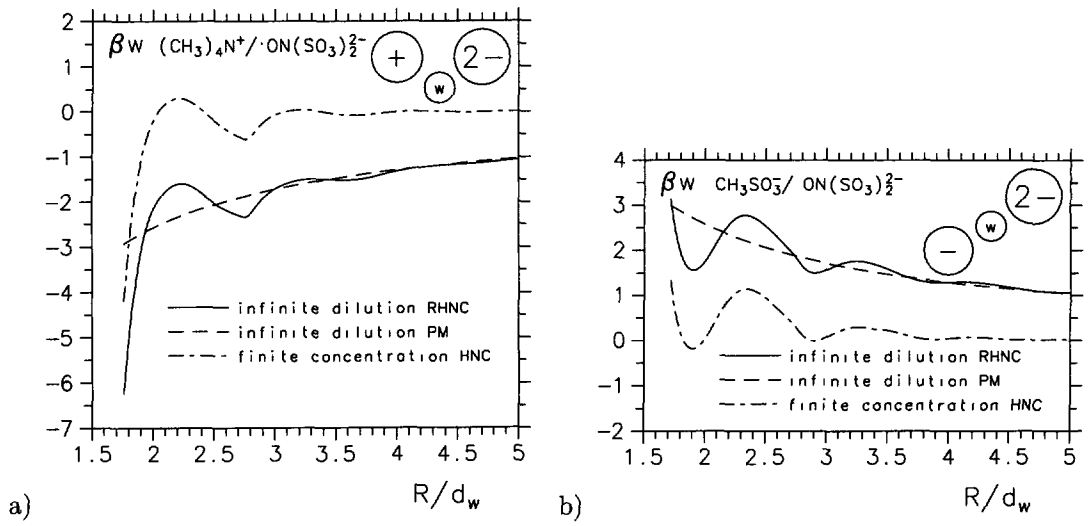

Fig. 5. — Behaviour of the ion-ion potentials of mean force *versus* the distance R between the ion centres for various theoretical approximations defined in Section 3: a) attractive pair $(CH_3)_4N^+/{}^{\bullet}ON(SO_3)_2^{2-}$, b) repulsive pair $(CH_3)SO_3^-/{}^{\bullet}ON(SO_3)_2^{2-}$ $d_w = 2.8$ Å is the diameter of the water molecule.

At any radical concentration c_S the relaxation rates for the attractive pair are about four times larger than those for the repulsive pair. Since the TMA^+ and MS^- ions nearly have the same self-diffusion constants, this effect results from the difference in the ion-ion PMF. Since the ions have similar diameters this difference is caused by the sign change of their Coulomb potential. Now, at the moderate ionic strengths studied here, the Coulomb forces are notably screened by the surrounding ions. The dimensionless PMF βw ($\beta = 1/k_BT$) of the pairs TMA^+/NDS^{2-} and MS^-/NDS^{2-} are displayed in Figure 5 as a function of the normalized ionic intercentre R/d_w, where d_w is the water diameter. The effective RHNC potentials βw_{IS}^{ID} in the infinite dilution limit, represented by continuous curves, are needed to calculate the HNC-PMF at finite concentration according to the procedure proposed in Section 3.3.1. As expected, when the interionic distance R increases, βw_{IS}^{ID} tends towards the dashed line of the primitive model (PM) recalled in Section 3.4. When the ions are in contact or close, their Coulomb potential is only partly screened by the water molecules coming in between. The values of βw_{IS}^{ID} are intermediate between those of the Coulomb potential *in vacuo* and those of the primitive model which describes the ions as two charged spheres in a dielectric continuum. When the interionic distance increases, βw_{IS}^{ID} shows marked oscillations with a period approximately equal to the water diameter. As soon as the thickness of the hydration shell separating the ions exceeds one or two water diameters d_w, there is no significant difference between the RHNC values and the primitive model. This means that the local structure formed by the water molecules around the ions mostly disappears beyond the first hydration shell. The HNC-PMF βw_{IS}^{FC} at finite concentration are represented by dash-dotted curves. They are equal to zero for $R \geq 4d_w$, which indicates a complete screening of the Coulomb forces between the two studied ions by the other ions in the solution. At very short distances, for both the attractive and repulsive pairs, the absolute values of βw_{IS}^{FC} are about 50% smaller than their infinite dilution counterparts. Nevertheless, the remaining difference between the attractive and repulsive βw_{IS}^{FC} *is sufficient* to accounts for the much larger relaxation rates of the attractive pair.

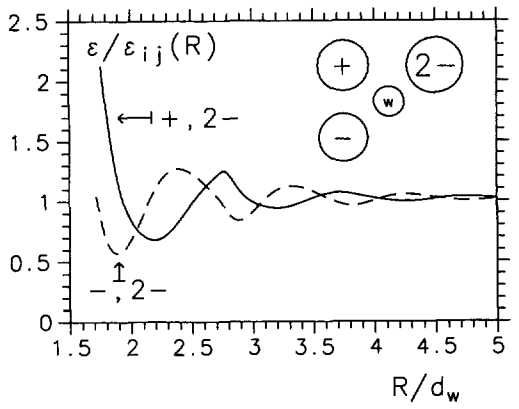

Fig. 6. — The inverse of the local dielectric constant $\varepsilon_{ij}(R)$, defined by equation (20), *versus* the ion-ion intercentre distance R for the attractive pair $(CH_3)_4N^+/^{\bullet}ON(SO_3)_2^{2-}$ and for the repulsive pair $(CH_3)SO_3^-/^{\bullet}ON(SO_3)_2^{2-}$ d_w is the water diameter. $\varepsilon = \lim_{R\to\infty} \varepsilon_{ij}(R)$ is the usual macroscopic dielectric constant.

Finally, the inverses of the local dielectric constants $\varepsilon/\varepsilon_{IS}(R)$, defined by equation (20), are reported in Figure 6 *versus* the interionic distance R, both for the attractive and repulsive ions, the infinite dilution PMF of which are shown in Figure 5. At the contact distance $b = (d_I + d_S)/2$, $\varepsilon_{IS}(b) \approx \varepsilon/2$ for the attractive pair because of the incomplete screening of the Coulomb potential by the water molecules of finite sizes. On the other hand, $\varepsilon_{IS}(b) \approx \varepsilon$ for the repulsive ions. This results from the competition between an enhancement of their Coulomb repulsion related to the incomplete water screening and the general opposite tendency of discrete solvent molecules to push two solutes in contact, as shown by the contact values taken by the pair distribution of two neutral solutes, which is notably larger than unity [49].

5.4. The $TMP^+/Mn(D_2O)_6^{2+}$ Repulsive Pair. — Finally, the pair of repulsive ions TMP^+ and $Mn(D_2O)_6^{2+}$ was investigated at 298 K in D_2O solutions containing 0.1 M of TMPCl and concentrations of $MnCl_2$ varying between 0 and 0.08 M. The proton resonance frequency of the TMP^+ methyl protons was $\nu_I = 200$ MHz. The experimental relaxation rates R_{1S} are given in Table VI.

Table VI. — *Measured relaxation rates R_1 of the protons on the $(CH_3)_4P^+$ ions for various concentrations c_S of hydrated paramagnetic ions $Mn(D_2O)_6^{2+}$ in D_2O solutions at 298 K. The concentration of diamagnetic tetramethylphosphonium chloride is $[(CH_3)_4PCl] = 0.1\,M$. The proton resonance frequency is $\nu_I = 200\,MHz$.*

$[MnCl_2]$ (M)	0	0.02	0.04	0.06	0.08
R_1 (s^{-1})	0.120	12.3	26.1	39.1	57.1

Geometrical and dynamical parameters of the various ions involved in the solutions are summarized in Tables I and II. The TMP^+ self-diffusion coefficient is $D_I^t = 0.87 \times 10^{-5}\,cm^2\,s^{-1}$. The $Mn(D_2O)_6^{2+}$ self-diffusion coefficient was determined according to the procedure of Section 5.1 using TMP^+ as the reference ion. It is $D_S^t = 0.50 \times 10^{-5}\,cm^2\,s^{-1}$

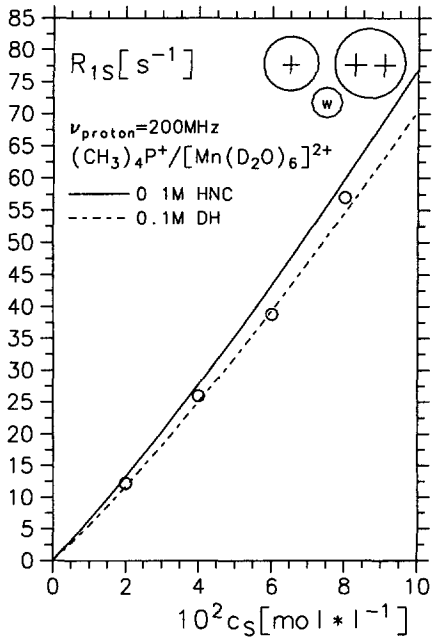

Fig. 7. — Intermolecular relaxation rates of the $(CH_3)_4P^+$ protons at 200 MHz *versus* the concentration c_S of paramagnetic $Mn(D_2O)_6^{2+}$ transition metal cations in a D_2O solution at 298 K. The concentration of $(CH_3)_4PCl$ is 0.1 M. The experimental results are compared with the HNC (continuous curve) and Debye-Hückel (dashed curve) approximations.

In Figure 7, the measured relaxation rates are compared with the theoretical values calculated from both the Debye-Hückel approximation and the HNC theory of Section 3.3.1. For this rather low ionic strength both methods predict the observed rates with excellent accuracy.

5.5. Influence of the Sizes of the Surrounding Ions. — In Section 5.1 a simplified treatment was suggested for the ions which surround the interacting ions and belong to different species. All the surrounding ions with the same charge have been replaced by ions of an effective species, the number density and diameter of which are defined by equations (28) to (30). The error induced by this approximation can be estimated by studying how the diameters d_k of the effective species influence the PMF. To this end, the HNC-PMF were calculated when the ions are in contact, both for the attractive and repulsive pairs, TMA^+/NDS^{2-} and MS^-/NDS^{2-}, studied in Section 5.3. It was found that increasing d_k by 10% leads to a relative variation of $\beta w_{ij}^{FC}(b)$, which is less than 1% for the two pairs in the limit $c_S \to 0$. At higher radical concentration $c_S = 0.1$ M, this variation remains of the order of 1%. To sum it up, there is no appreciable change of the PMF. The short range indirect spatial correlations between the interacting ions weakly depend on the sizes of the surrounding ions up to moderate concentrations. The latter can then be safely replaced by effective species as suggested in this paper.

5.6. Influence of the Indirect Short Range Spatial Correlations of the Surrounding Ions. — The HNC and RHNC approximations of Sections 3.3.1 and 3.3.2 are expected to lead to very close results. Indeed, the purely ionic reference system without

water is rather dilute so that there are only weak spatial correlations among the ions. Thus, the functions η_{rij}^{ion} and w_{rij}^{ion} are almost negligible. The RHNC closure (17) tends towards the HNC closure (15) so that the RHNC potential w_{ij}^{FC}, defined by (16), is nearly identical to the HNC value (13). This can be checked for the ion pairs TMA^+/NDS^{2-} and MS^-/NDS^{2-}, in the solutions studied in Section 5.3. When $c_S \to 0$, the PMF values $\beta w_{ij}^{FC}(b)$, calculated at the contact intercentre distance b for the HNC and RHNC approximations, differ by 0.15 and 0.7% for the attractive and repulsive ions, respectively. For $c_S = 0.1$ M, the corresponding changes of the PMF values remain of the order of 1%.

6. Conclusion

The microdynamics of a large variety of pairs of diamagnetic and paramagnetic ions has been investigated in heavy water solutions up to moderate ionic strengths. We have developed a new approach to calculate the potentials of mean force $w_{ij}^{FC}(R)$ between two ions of species i and j at finite ionic concentrations (FC). In this approach all the ions are treated as discrete particles. Each w_{ij}^{FC} is the sum of the infinite dilution (ID) effective potential w_{ij}^{ID} and of a corrective term which results from the indirect spatial correlations with all the other ions coupled by their own infinite dilution effective potentials. This theory goes beyond the Debye-Hückel screening approximation where the surrounding ions are represented by a continuous charge distribution. The measured intermolecular relaxation rates of the protons on the diamagnetic ions interacting with the electronic spins of the paramagnetic ions are well-predicted by our models of solutions and by our theoretical approach. For all the studied ion pairs the agreement is very satisfactory for the numerous ionic concentrations and proton NMR resonance frequencies. This justifies the method proposed in Section 2.3.3 to determine the self-diffusion coefficient of paramagnetic ions from the intermolecular relaxation rates, even if some care should be taken when the ion electric charge is distant from the ion centre (see Sect. 5.3). For the present experiments, the refined HNC theory does not significantly improve on the simpler Debye-Hückel screening model, even for attractive ions which are often close and for which an accurate treatment of the interactions with the surrounding ions is expected to be necessary. The Debye-Hückel screening approximation can be reasonably used up to ionic strengths ≈ 1 M, at least for solvents, such as water, with high dielectric constants. In particular, this allows the theoretical treatment of anisotropic charged species at the Debye-Hückel level, which represents a considerable simplification with respect to the complex computations needed to solve the HNC theory for coupled anisotropic charged particles. The success of the Debye-Hückel screening model can be understood as follows. The decisive progress comes from the potentials of mean force at infinite dilution which are obtained at the Born-Oppenheimer level consisting in treating the water molecules and the ions as discrete particles. Compared to this improvement with respect to the primitive model [8], the difference between the Debye-Hückel screening by a continuous charge distribution and the HNC screening by discrete surrounding ions is of minor importance at these moderate ionic strengths. Thus, a further stage will be to apply the various theories discussed in this paper to much more concentrated ionic solutions, and to compare and check the accuracy of their predictions. Complementary scattering results would be helpful to check the reliability of our method which mixes a Born-Oppenheimer theory at infinite dilution with a sort of McMillan-Mayer approach [17b] to take the ionic concentration into account.

Acknowledgments

We are indebted to Dr M. Holz for having favoured the cooperation between our groups in Bari and Grenoble. The suggestion of Prof. P. Turq to develop the present approach to calculate the ion-ion potentials of mean force is greatly acknowledged.

References

[1] Torrey H.C., *Phys. Rev.* **92** (1953) 962.
[2] Albrand J.P., Taïeb M.C., Fries P.H. and Belorizky E., *J. Chem. Phys.* **78** (1983) 5809.
[3] Odelius M., Laaksonen A., Levitt M.H. and Kowalewski J., *J. Magn. Reson. A* **105** (1993) 289.
[4] Holz M., *Prog. NMR Spectroscopy* **18** (1986) 27.
[5] Müller K.J. and Hertz H.G., *Chem. Script.* **29** (1989) 277.
[6] Stark U. and Müller-Warmuth W., *Ber. Bunsenges. Phys. Chem.* **94** (1990) 168.
[7] Coolbaugh Lester C. and Bryant R.G., *J. Phys. Chem.* **94** (1990) 2843.
[8] Fries P.H., Belorizky E., Bourdin N., Cinget F., Gagnaire D., Gorecki W., Jeannin M. and Vottéro Ph., *J. Molec. Struct. Theochem* **330** (1995) 335.
[9] Sacco A., *Chem. Soc. Rev.* **23** (1994) 129.
[10] Sacco A., Asciolla A., Matteoli E. and Holz M., *J. Chem. Soc., Faraday Trans.* **92** (1996) 35.
[11] Göller R., Hertz H.G. and Tutsch R., *Pure Appl. Chem.* **32** (1972) 149.
[12] Kowalewski J., Nordenskiöld L., Benetis N. and Westlund P.O., *Prog. NMR Spectroscopy* **17** (1985) 141.
[13] Jeannin M., Belorizky E., Fries P.H. and Gorecki W., *J. Phys. II France* **3** (1993) 1511.
[14] Belorizky E., Fries P.H., Gorecki W., Jeannin M. and Roby C., *J. Phys. Chem.* **98** (1994) 4517.
[15] Berry R.S., Rice S.A. and Ross J., Physical Chemistry (Wiley, New York, 1980) (a) pp. 997-1006; (b) Table II.3, p. 449.
[16] Hansen J.P. and McDonald I.R., Theory of Simple Liquids (Academic Press, London, 1986) pp. 97-121.
[17] Friedman H.L., A Course in Statistical Mechanics (Prentice-Hall, London, 1985) (a) pp. 111-156; (b) pp. 201-213.
[18] Kay R.L. and Evans D.F., *J. Phys. Chem.* **69** (1965) 4216.
[19] Atkins P.W., Physical Chemistry (Oxford University Press, Oxford, 1992) (a) pp. 748-766; (b) pp. 225-237 and pp. 951-952.
[20] Moore W.J., Chimie Physique (Dunod, Paris, 1965) pp. 382-404.
[21] Hertz H.G., Lindman B. and Siepe V., *Ber. Bunsenges. Phys. Chem.* **73** (1969) 542.
[22] Bradl S., Lang E.W., Turner J.Z. and Soper A.K., *J. Phys. Chem.* **98** (1994) 8161.
[23] Harned H.S. and Owen B.B, The Physical Chemistry of Electrolytic Solutions (Reinhold, London, 1964) pp. 244-245.
[24] Raspi G., Cinquantini A. and Cospito M., *Electroanalytical Chem. Interfacial Electrochem.* **59** (1975) 69.
[25] Bernard O., Kunz W., Turq P. and Blum L., *J. Phys. Chem.* **96** (1992) 398.
[26] Stejskal E.O. and Tanner J.E., *J. Chem. Phys.* **42** (1965) 288.

[27] Terazima M., Tenma S., Watanabe H. and Tominaga T., *J. Chem. Soc., Faraday Trans.* **92** (1996) 3057.
[28] Levy G.C. and Peat I.R., *J. Magn. Reson.* **18** (1975) 500.
[29] Jeannin M., PhD Thesis (Grenoble, 1994).
[30] Fries P.H. and Patey G.N., *J. Chem. Phys.* **80** (1984) 6253.
[31] Kusalik P.G. and Patey G.N., *J. Chem. Phys.* **88** (1988) 7715.
[32] Fries P.H., Kunz W., Calmettes P. and Turq P., *J. Chem. Phys.* **101** (1994) 554.
[33] Carnie S.L. and Patey G.N., *Molec. Phys.* **47** (1982) 1129.
[34] Patey G.N. and Carnie S.L., *J. Chem. Phys.* **78** (1983) 5183.
[35] Lado F., *J. Chem. Phys.* **135** (1964) 1013.
[36] Holmberg R.W. and Wilson B.J., *J. Chem. Phys.* **61** (1974) 921.
[37] Abragam A. and Bleaney B., Résonance Paramagnétique Électronique des Ions de Transition (PUF, Paris, 1971) pp. 432-438.
[38] Pilbrow J.R., Transition Ion Electron Paramagnetic Resonance (Clarendon, Oxford, 1990) pp. 1-31.
[39] Kooser R.G., Volland W.V. and Freed J.H., *J. Chem. Phys.* **50** (1969) 5243.
[40] Rubinstein M., Baram A. and Luz Z., *Mol. Phys.* **20** (1971) 67.
[41] Guéron M., *J. Magn. Reson.* **19** (1975) 58.
[42] Banci L., Bertini I. and Luchinat C., Nuclear and Electron Relaxation (VCH, Weinheim, 1991) pp. 101-103.
[43] Fries P.H., Belorizky E., Rendell J.C.T., Burnell E.E. and Patey G.N., *J. Phys. Chem.* **94** (1990) 6263.
[44] Ayant Y., Belorizky E., Fries P.H. and Rosset J., *J. Phys. France* **38** (1977) 325.
[45] Fries P.H. and Belorizky E., *J. Phys. France* **39** (1978) 1263.
[46] Abragam A., Les Principes du Magnétisme Nucléaire (PUF, Paris, 1961) pp. 267-306.
[47] Fries P.H., Jagannathan N.R., Herring F.G. and Patey G.N., *J. Chem. Phys.* **80** (1984) 6267.
[48] Jander G., Blohm Chr. and Grüttner B., *Z. Anorg. Chem.* **258** (1949) 205.
[49] Fries P.H. and Hansen J.P., *Molec. Phys.* **48** (1983) 891.